Journal of the Korean Society of Oceanography
Vol. 38, No. 3, pp. 122 — 134 September 2003

Observations of Coastal Upwelling at Ulsan in summer 1997

JAE CHUL LEE*, DAE HYUN KIM, AND JEONG-CHANG KIM
Korea Inter-university Institute of Ocean Science, Pukyong National University, Busan 608-737, Korea

Low-pass filtered time series of wind, coastal temperature, sea level and current were analyzed to understand the coastal upwelling processes in the southeast coast of Korea. Southerly winds favorable for coastal upwelling were dominant in summer of 1997. Total period of four major wind events amounts to 58 days during one hundred days from June to early September. Coastal temperature is most sensitive to variations of wind. The time lag between the onset of southerly (northerly) winds and decrease (increase) of temperature is 3–18 hours. In the frequency domain the coherent bands have periods of 2.4 and 4.0–5.4 days with respective phase lags of 17 and 27–37 hours. Despite the sensitive response, the magnitude of temperature change is not quantitatively proportional to the intensity or duration of the wind, because it depends on the degree of baroclinic tilting of isotherms built dynamically by the strong Tsushima Warm Current (TWC). Current is particularly strong near the coast and has a large vertical shear during the upwelling periods, which is associated with the baroclinic tilting. Both of current and sea level are poorly coherent with wind or temperature except for the period of 4 days.

Key words: Coastal Upwelling, Tsushima Warm Current, Sea Surface Temperature, Sea Level, Coherence

INTRODUCTION

It is well known that cold water mass appears off the southeast coast of Korea near Ulsan in summer. Using the hydrographic data, An (1974) and Lee (1978) showed the presence of the cold water mass. Lee (1983) compared the time series of winds, coastal water temperatures and sea levels along the southeast coast to prove that the appearance of cold water was due to the southerly wind prevailing in summer. Sea surface temperature (SST) began to decrease 1–2 days after the onset of the upwelling-favorable wind that lasted three days or longer. Lee and Na (1985), using the same time series data and mean bottom temperature, suggested the contribution of baroclinic tilting of intensified Tsushima Warm Current (TWC) and the diverging isobaths off Busan to Gampo. All of the previous research used the bimonthly hydrographic data and daily coastaltemperature by National Fisheries Research and Development Institute (NFRDI). Byun (1989) studied the effects of coastal topography as well as the wind at Busan. Lee *et al.* (1998) also compared the same daily SST data with SSM/I winds to yield the results that 80% of southwesterly wind events caused the SST to drop more than 1°C and that the response time was less than two days.

In the foregoing studies, the resolution of analysis was limited by the time interval of daily SST data. Hourly data of winds and sea levels were converted to the daily mean values accordingly to be compared with SST. Rough estimate of two days for the response time should be refined by more elaborate observations. Moreover, the current was not observed long enough to resolve the subinertial variability although the current condition is indispensable for upwelling process. For this improved study, we deployed a tide gauge and a current meter during the summer of 1997. Along with the CTD observation and satellite infrared images, the finer time series are used to give more detailed results about the upwelling processes.

OBSERVATIONS AND METHODS

As a beginning stage of multi-year program for upwelling studies, we deployed a tide gauge (SBE 26, Sea-Bird Electronics) and a current meter (RCM-9, Aanderaa Instruments) in order to obtain the time series. Tide gauge was installed at the bottom of coastal area north of Ulsan where the water depth was about 15 m (Site H in Fig. 1). Current meter

*Corresponding author: jaechul@pknu.ac.kr

was moored at 20 m depth of Site M with total depth of 110 m, 11 km distant from the coast. The observations began on 4 June 1997 with sampling interval of 10 and 20 minutes for current and sea level, respectively. Although the instruments were deployed until early September, the current data was not available after 31 July because the bad data began to be recorded for unknown reason. Hourly wind data from the meteorological station at Busan was used.

CTD and ADCP observations were conducted twice by R/V Tamyang equipped with SBE 911 plus (Sea-Bird Electronics) and V/M ADCP (150 kHz Narrow Bands, RD Instruments). On 4 June, Line-A off Ulsan was observed right after the mooring of current meter and Line-A, B, C were covered on 24 June. CTD observation was carried out from the coast to the offshore direction, then continuous ADCP sections were obtained by traversing back toward the coast along each line. Hydrographic data of NFRDI observed in August were also used.

For the analyses of vector data of wind and current, alongshore and offshore components were separated by rotating the local coordinate systems 22.5° in clockwise direction (Fig. 1). This angle of rotation is not only the same as that of Lee (1983) but also is validated by the principal component analysis of the current data. Since the subtidal process is of foremost interest, all the time series data were low-pass filtered by Butterworth Filter with 40-hour cutoff frequency then compared with each other in the time domain. For closer investigation in the frequency domain the coherence analyses were also carried out.

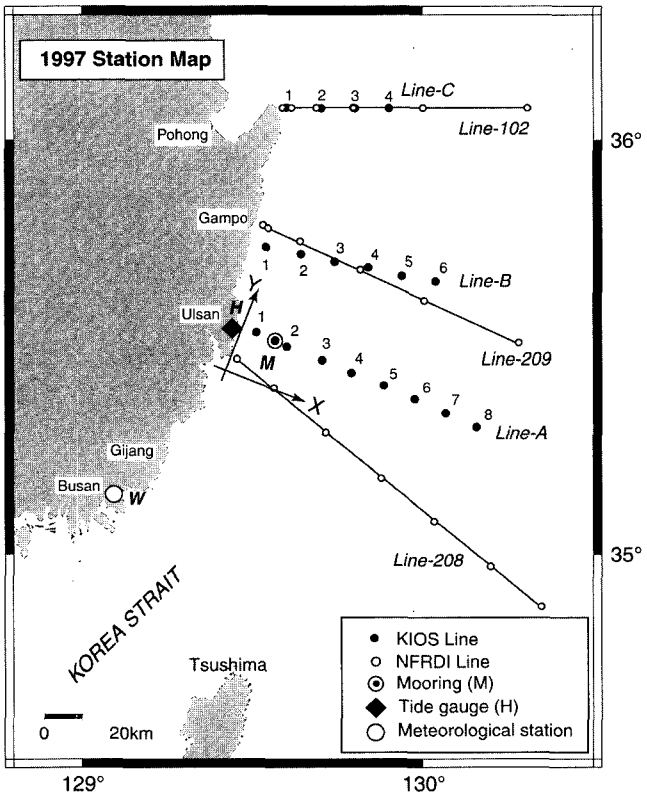

Fig. 1. Positions of hydrographic observation (KIOS lines and NFRDI lines), current meter mooring (M), tide gauge (H) and meteorological station (W). Y-axis in the local coordinate system is parallel to the coast at Ulsan.

We could procure eight NOAA images of good quality from the Agriculture, Forestry and Fisheries Research Information Center of Japan. These IR images are reviewed in order to get a general picture about the coastal upwelling in the research area. Daily SST data at Gijang, Ulsan and Gampo by NFRDI were also used to investigate the changes of the coastal temperature in the southeast coast.

SATELLITE INFRARED DATA

Eight IR pictures of acceptable quality were available during the upwelling season from June through August (Fig. 2). All of the pictures reveal that coastal upwelling occurred frequently so that low SST in the southeast coast is a prominent feature in the summer of 1997. On 23 June, two days after the onset of the southwesterly wind (cf. Fig. 10) a narrow strip of relatively low temperature from Busan to Gampo signifies the early stage of coastal upwelling. The cold water of decreased temperature to about 16°C on 28 June, located to the north of Ulsan, has two branches; one extending westward to Pohang and the other eastward into the East Sea. The pattern of cold water distribution is still not changed by 3 July but the extended part suggests the growing stage of a new event. It will be illustrated in later time-series part (Fig. 10) that a short period of intense northeasterly wind is related with the image on 28 June whereas the date 3 July corresponds to the middle of the stronger upwelling period. In spite of the cloud coverage, it is not difficult to presume that the cold water regime would include a part of clouded area south of Ulsan. Upwelling appears to decay on 18 July and the cold water having a narrow band from the southwest of Busan to Ulsan occupies a wide area off the east coast where the temperature of its central part is about 20°C.

The SST is generally much higher in August compared to the preceding months. A small scale upwelling is formed between Busan and Ulsan on 22 August then decayed on 24 when a cold water mass detached from

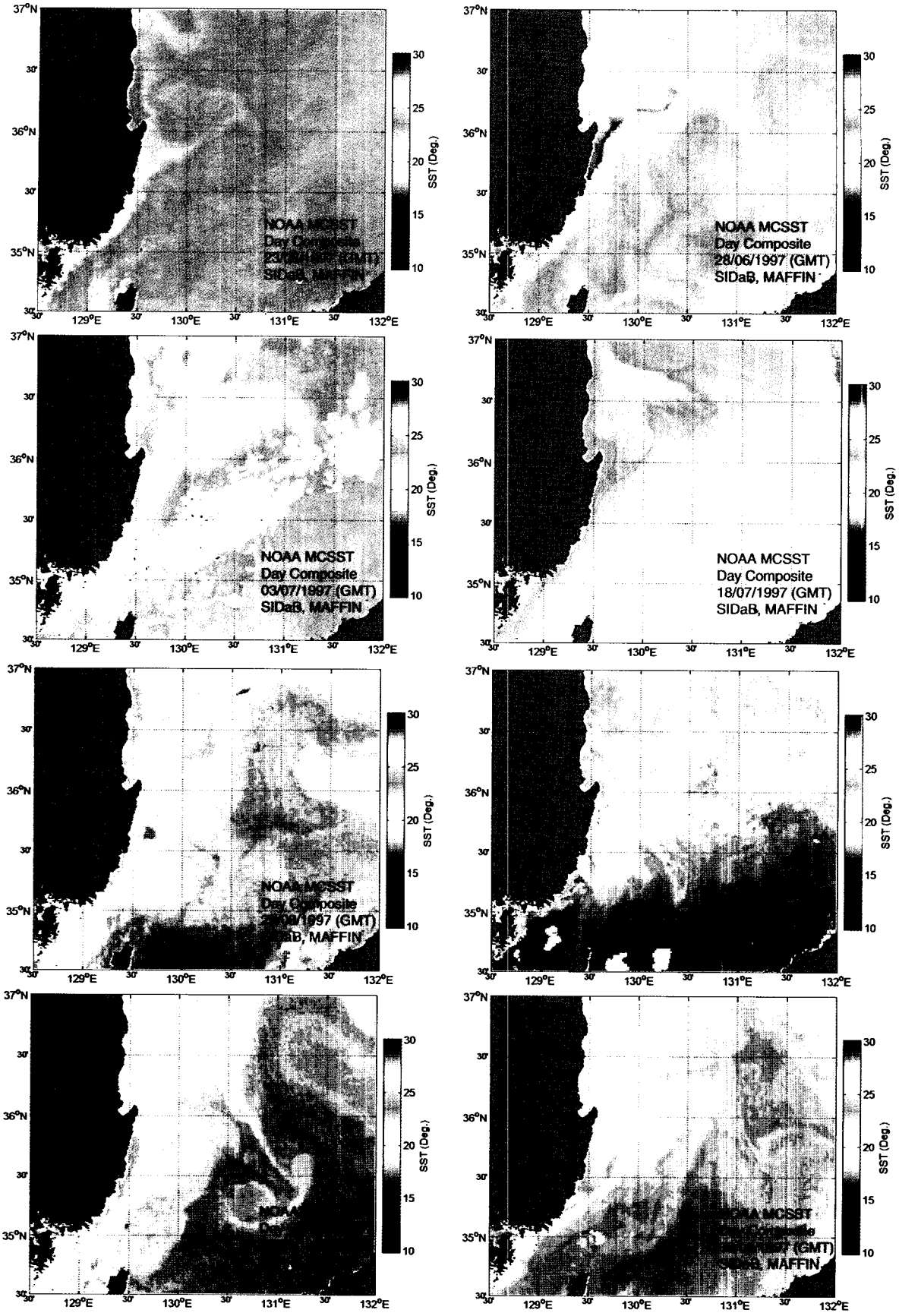

Fig. 2. Satellite infrared images during summer of 1997.

the coast makes a cyclonic eddy. The images of 28 and 30 August demonstrate another process of developing and extending of cold water, respectively. Based on these limited number of IR images we can recognize that the upwelling was frequent and active during summer 1997.

DAILY SST DATA

Fig. 3 is the time series of daily coastal temperature at three stations observed by NFRDI, same kind of data as those used in the previous papers. Gijang is a northern part of Busan. It is discernible that the temperature changes at three stations in nearly the same manner. There are extended periods of decreasing temperature. Acknowledged are at least three extended periods of decreasing temperature as indicated by the horizontal arrows on Fig. 3; first event from 21 June to 7 July, second from 2 to 12 August, and the last from 27 August to 3 September. There are also many occasions of shorter periods.

The amount of temperature decrease is greatest at Gampo as described by Lee (1983) and smallest at Gijang in most cases. In case of the first event, temperature begins to drop later at Gampo than at southern stations but the magnitude of decrease amounts to 11°C in 16 days. This result may be reasoned from the IR images that the upwelling begins near Ulsan but the center of the cold water moves to Gampo in the most developed stage then the decaying process follows. Temperature at Gampo begins to decrease later in the second event too, but the process is much more intense with a greatest drop of about 14.0°C despite the shorter period of 10 days.

It is possible to figure out roughly the major upwelling-downwelling events from these daily records of SST. But in this paper we can take a closer look at the detailed variability using the finer time series as given in the last section.

WIND AND CURRENT CONDITIONS

Stick vector plots for the low-pass filtered wind and current at Site M are presented at 4-hour interval (Fig. 4) in order to provide a perspective on the general conditions associated with upwelling.

Wind is rather weak in early June but begins to get stronger in late June and becomes a little weaker again in September. Northeastward wind favorable for upwelling is comparatively dominant. Maximum and average wind speed is 10.8 m/sec and 3.3 m/sec, respectively.

The current to the NNE direction is predominant during the whole period of 56 days undoubtedly due to the influence of the TWC. Mean and standard deviation of current speed are 61.4 cm/sec and 17.3 cm/sec respectively. Maximum speed is 104.1 cm/sec while the total velocity including the tidal current is 156.0 cm/sec on 20 July. Because of the steadiness and greater strength, the low frequency current is more dominant than tidal current. The current becomes particularly weaker twice in the first half of June and late August. Current direction changes eastward in 2–3 days then the original NNE direction is restored soon. Including the two periods of weak velocity, the fluctuations of current do not seem to be influenced by the wind.

Fig. 5 is a scatter plot of total velocity also showing the average velocity of 60.8 cm/sec as well as the standard deviation ellipse derived from the principal component analysis. Northeastward velocity is predominant. The semi-major axis of the ellipse is in NNE direction (22.5° from the north) and the velocity components to this direction contain 84% of total variance. Therefore, this direction is not only parallel to the southeast coast from Busan to Pohang but is the direction of the most dominant velocity.

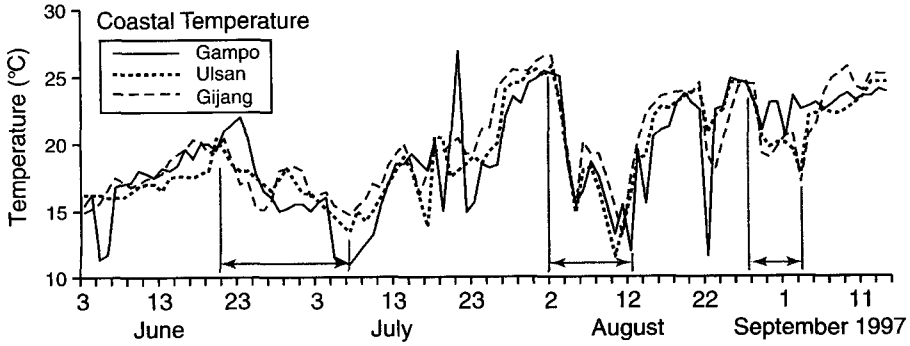

Fig. 3. Daily coastal SST at Gijang, Ulsan and Gampo in summer 1997.

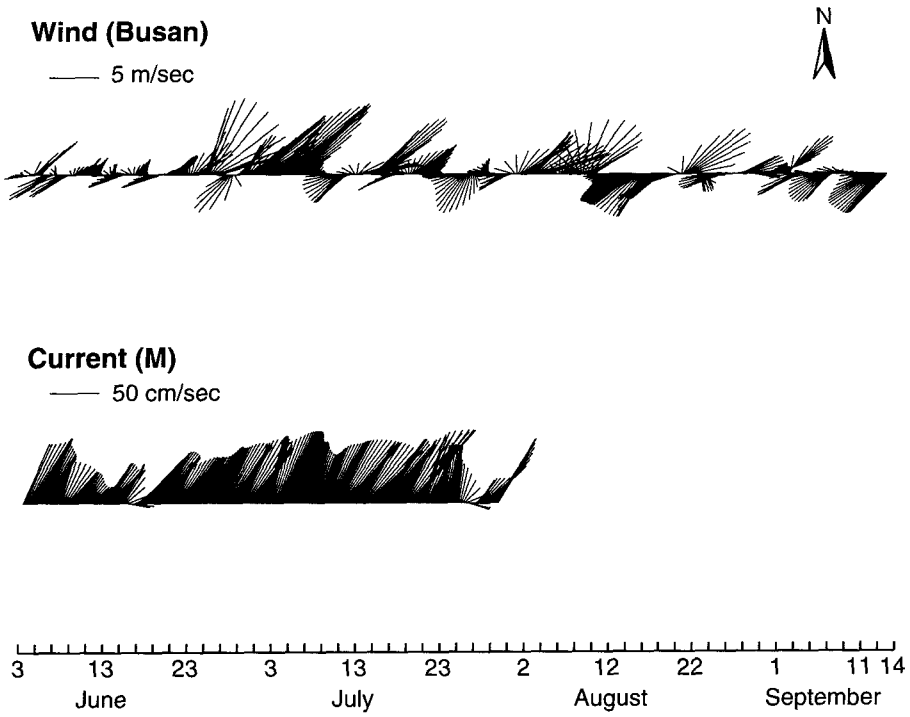

Fig. 4. Stick vector plots of wind at Busan (upper part) and current at the mooring site (lower part).

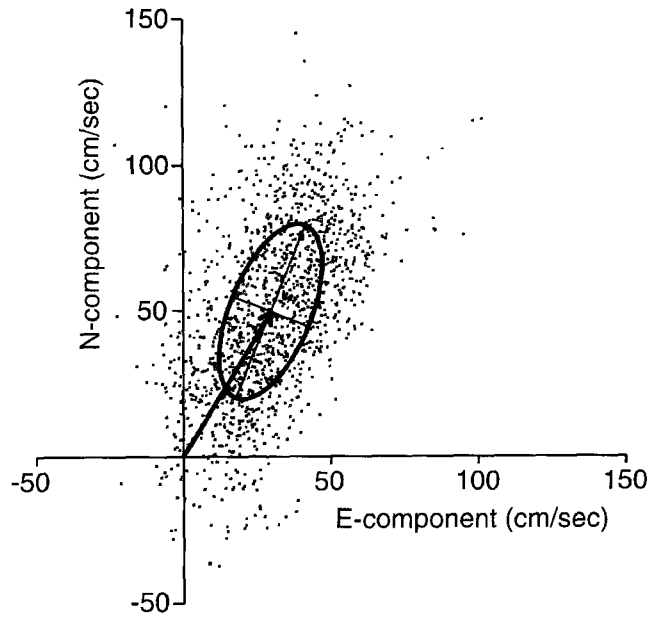

Fig. 5. Scatter diagram showing the distribution of observed velocity with its average and standard deviation ellipse of low-pass filtered velocity.

CTD OBSERVATIONS

Fig. 6 shows the horizontal distribution of temperature at the surface (upper part) and 20 m depth (lower part) in June (left part) and August (right part). Low temperature with a center less than 17°C at Ulsan on 24 June is a typical evidence of coastal upwelling. This figure can be compared with an IR image of 23 June (Fig. 2). Cold water mass below 15°C resides at 20 m depth of the coastal area. Low temperature is not discernible at the surface of Ulsan-Gampo region in August, although a center of cold water (lower than 13°C) still remains at Gampo. Curvature of 25°C isotherm at the surface implies an offshore extension of relatively cold water but the cyclonic motion of detached cold water as illustrated in IR image of 24 August is not resolved by the observation.

Cross sections (Fig. 7) are particularly helpful to understand the hydrographic conditions. Cold water of lower layer ascends toward the coast, which is a direct indication of upwelling. Cold bottom water below 3°C appears in early June (Fig. 7a). The depth of 10°C isotherm is shallower than 40 m near the coast. Considering that the two observations were conducted in the early phase of upwelling events, we can expect a cold water mass to ascend to the surface during the intense processes. A common characteristic of interest for the salinity sections is that the upper and lower layers are divided by high salinity water greater than 34.3 psu at 20–60 m depth near the coast. The corresponding temperatures of this Tsushima Current Intermediate Water are 15–18°C in

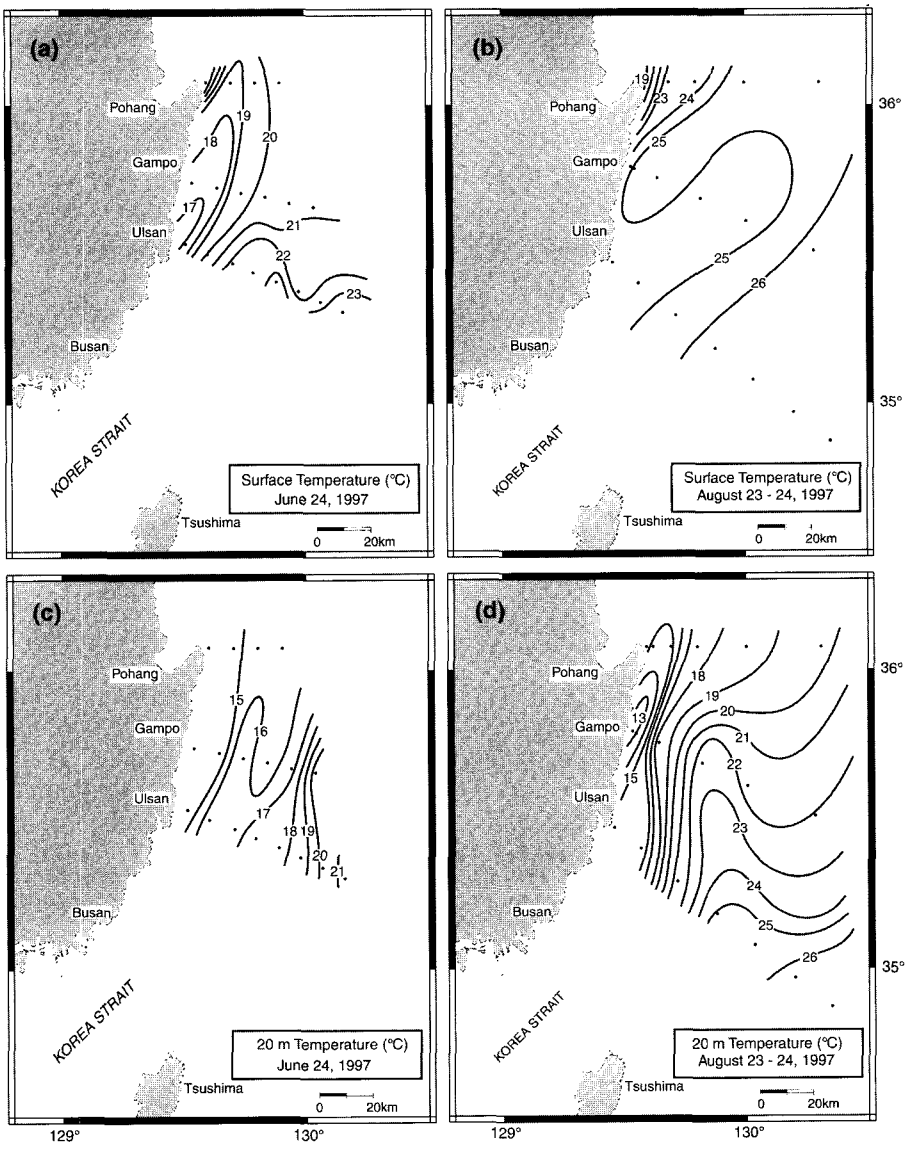

Fig. 6. Horizontal distribution of temperature at surface (upper parts) and 20 m depth (lower parts).

early June and 12–17°C in late June.

In the cross section of Line-B off Gampo (Fig.7 e and f), temperature and salinity in deeper layer are lower (below 3°C and 34.05 psu) than those in the southern section of Line-A off Ulsan (Fig. 7c and d). At the same depth of 100 m, temperature is 7°C at A2 and 3°C at B2. This implies that the cold water mass off Ulsan may originate from the north. These hydrographic conditions enable us to consider the two-layer structure with a southward undercurrent. However, the presence of the undercurrent has not been verified by the direct observation of current yet. Both of isotherms and isohalines are nearly horizontal or descending toward the coast between stations B1 and B2, which suggest the presence of a southward flow as shown in the velocity distribution (Fig. 8).

CROSS SECTIONS OF ALONGSHORE VELOCITY

Continuous ADCP sections were collected in every return cruise toward the coast after the CTD observation was made along each line. Because the significant contribution of tidal current changing with time as well as distance is inherent in the data, this effect must be eliminated for acceptable interpretation. Fortunately we have a time series of current and the information of distance-dependent velocity distribution is available from the observations by Teague *et al.* (2001).

Left parts of Fig. 8 are the sections of observed alongshore velocity containing the influence of tidal current. Tidal velocity curves are inserted in each fig-

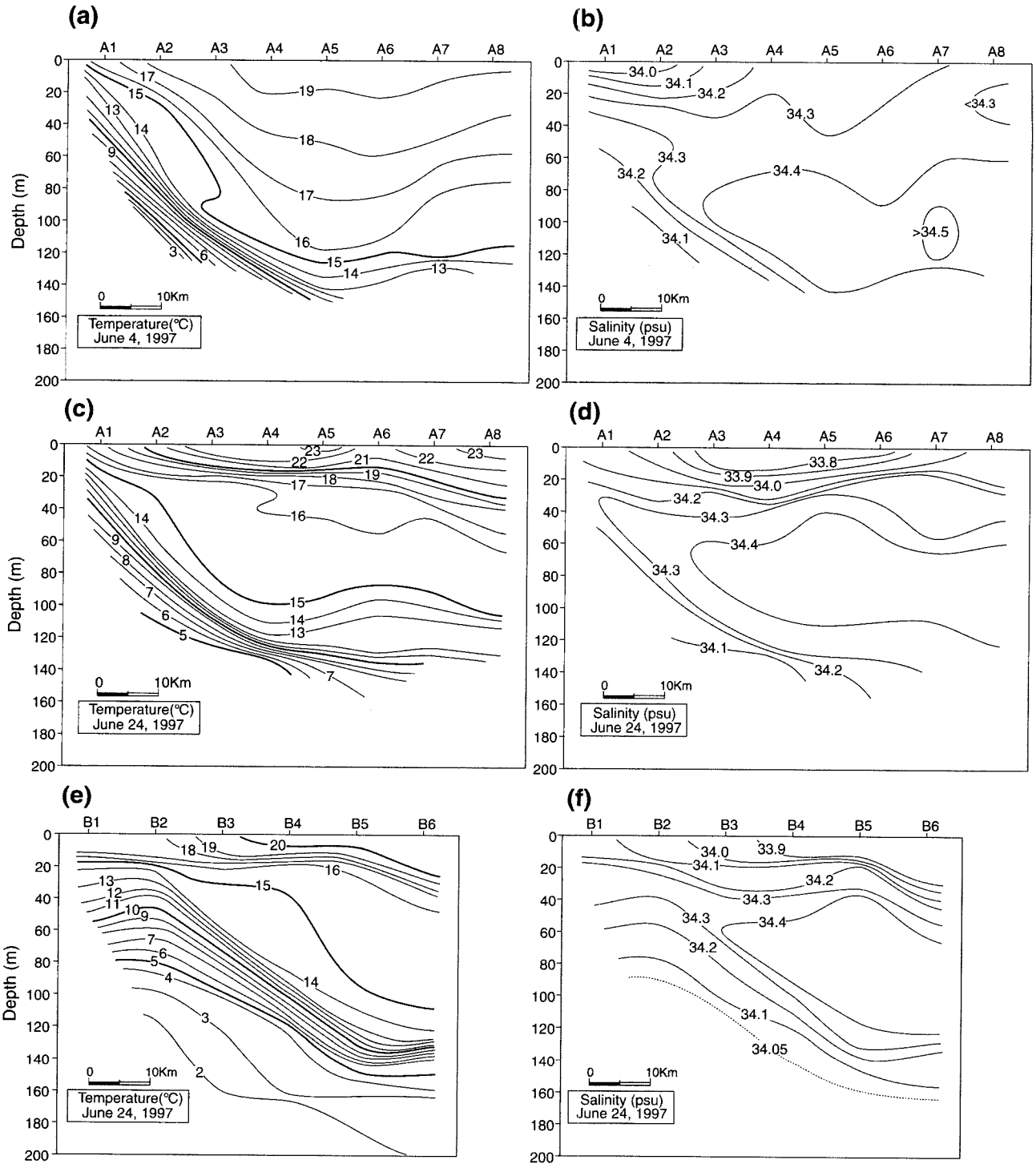

Fig. 7. Vertical distribution of temperature (left) and salinity (right) along Line-A and Line-B.

ure where the shaded bars represent the time of observation. Because the ship moved toward the coast, the left ends of bars correspond to the beginning of the sections at the offshore stations of A8 and B6. The constant ship speed with GPS data enables us to convert the curves of tidal current into the horizontal distributions. Because the amplitude of tidal current also varies with distance from the coast like the Kelvin waves, the horizontal distribution needs to be adjusted accordingly.

Teague *et al.* (2001) described the tidal current and Book *et al.* (2003) studied the data assimilation

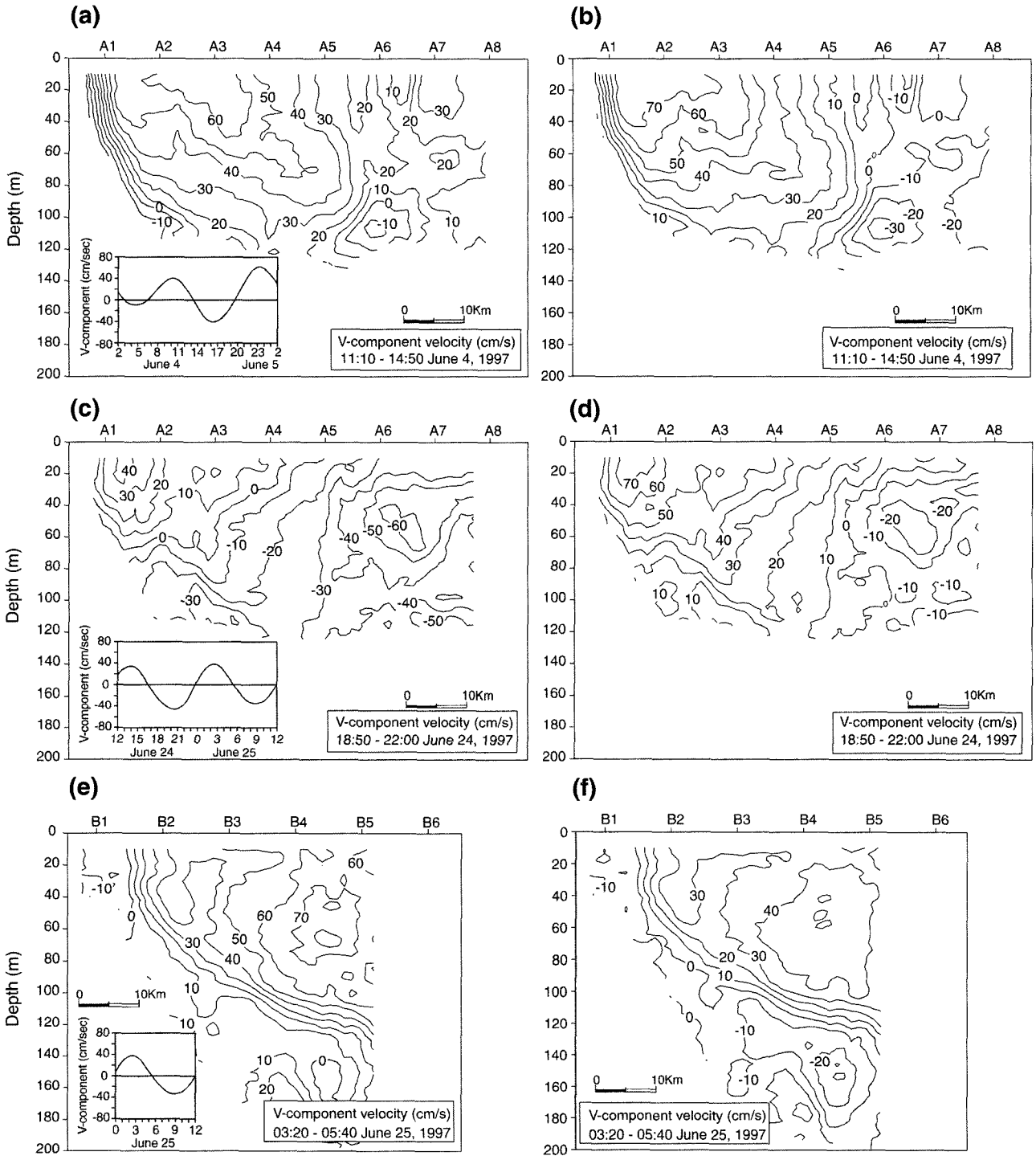

Fig. 8. Cross sections of alongshore velocity observed by V/M ADCP. Observed values are displayed in the left part with the inlets of tidal velocity curve where shaded bars represent the duration of observation. Right parts are the distributions of estimated nontidal velocity corrected by the observed current data.

model of tide using the ADCP data in the Korea Strait. The distribution of amplitude and phase of tidal current based on the analysis of Book *et al.* (2003) is shown in Fig. 9. Exponential curve fitting for the most dominant M_2 component shows that the amplitude decreases about 23% at the offshore side of the cross sections. The position of the smallest amplitude is close to the amphidromic point. Phase generally increases toward the offshore direction, but the phase lag within the velocity sections (Fig. 8)

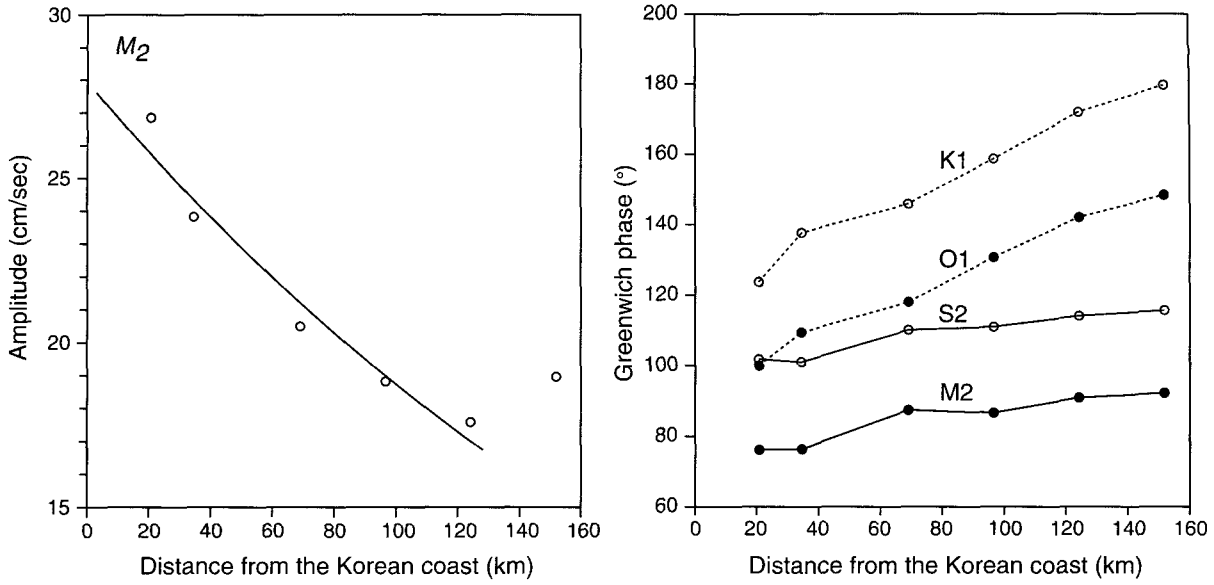

Fig. 9. Distribution of amplitude (left part) and phase (right part) of tidal current as a function of distance from the coast.

of about 70 km from the coast is negligibly small (about 20 minutes) for semidiurnal components. Although the diurnal components have larger lags, their contribution is relatively small. Therefore, the distance-dependent distribution of tidal velocity can be adjusted based on the exponential fitting of observed amplitude assuming that the tidal velocity decreases with distance like M_2 component does. This adjusted tidal current was subtracted from the observed velocity to extract the nontidal parts as shown in the right parts of Fig. 8. The same method is applied to the Section-B off Gampo under the inevitable assumption that the tidal current may not differ significantly from the Site M because the coastline is almost straight from Ulsan to Gampo and the distance is not large for the tidal scale. But the care is needed for interpretation of data.

It is remarkable that the current is particularly strong (greater than 80 cm/sec) and vertical difference is as great as 60 cm/sec near the Ulsan coast west of A3 (Fig. 8b and d). This dominant TWC with large velocity shear is of course responsible for the baroclinic tilting shown in Fig. 7. A weak southward flow at offshore stations of Line-A on 4 and 24 June may be due to the meandering branch of TWC as anticipated from the curvature of 22°C and 23°C isotherms in Fig. 6a, or the wake effect of the Tsushima Island (Teague *et al.*, 2001). However, stronger southward velocity in deeper layer on 4 June (Fig. 8b) is not likely to be the TWC that is usually stronger in the upper layer. This suggests a possibility of an extension of the undercurrent.

A weak southward coastal current is observed at the Section B off Gampo, as expected in the cross sections of temperature and salinity (Fig. 7e and f). TWC is weaker than in the Section A, and this is explained by the diverging isotherms in Fig. 6a. More striking thing is that there is an undercurrent below 100 m depth. This undercurrent is not found in the southern section on the same day probably because the strong TWC reaches the bottom near the coast. It is not certain from this data if this undercurrent stops before arriving at the Section A or shifts its path toward the offshore side. It seems possible that the undercurrent may develop in the southern section when the TWC becomes weak.

TIME SERIES ANALYSES

Hourly time series of low-frequency wind, current, sea level and temperature are compared in Fig. 10 in order to examine the processes of wind-induced upwelling. Dates of IR images and CTD observations are denoted on the time axis for easy comparison with Figs. 2, 6 and 7.

First graph of Fig. 10 is the record of wind at Busan. Positive alongshore component is dominant and there are several occasions of this upwelling-favorable wind that lasted extended period of time. It seems reasonable to group four major wind events favorable for upwelling as numbered on the figure. Brief episodes of downwelling-wind are included in each event, because such a

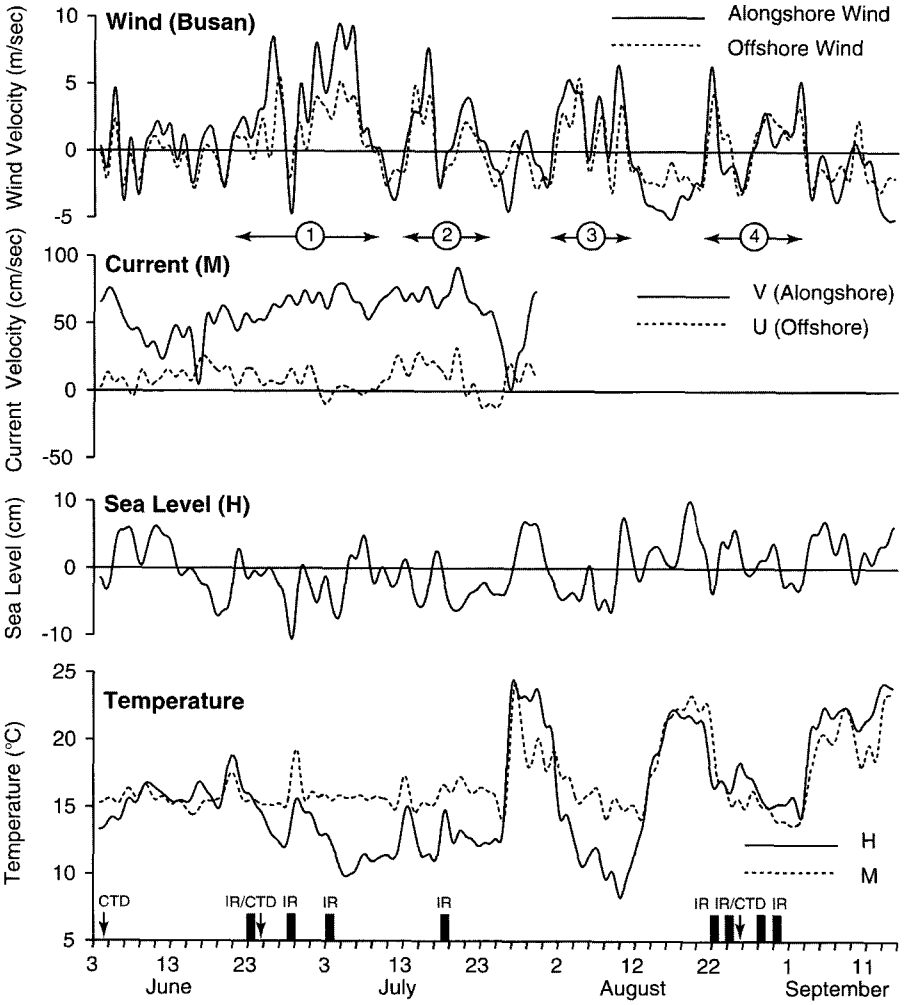

Fig. 10. Temporal variations of wind, current velocity, sea level and temperature. Four events of upwelling-favorable wind are denoted by the numbers in the shaded bars. The times of IR pictures used in Fig. 2 and CTD observations are marked at the bottom of the figure.

short impulse cannot remove the upwelling effect completely as proved by the temperature data. Major four events account for 58 days among one hundred days from June to early September.

Ekman dynamics predicts that temperature and sea level decrease and the coastal jet intensifies with upwelling-favorable wind near the coast. An excellent example is Smith (1974). These relations were already examined by Lee (1983) but are scrutinized again in this study by more refined data to yield more precise results. With a first look it is readily understood that the temperature responds most sensitively to the wind. Coastal site (H) has greater amplitude of variation than mooring site (M) has. Temperature decrease is very impressive during major events in spite of several instances of brief relaxation due to reduced or reversed winds.

However, the amount of temperature change is not quantitatively proportional to the wind. For example, temperature decreases 8.5°C by strong wind of Event 1 while it is about 10°C during shorter and weaker Event 2. It is striking that the coastal temperature can drop below 8°C during an intense upwelling like in August. Moreover, two downwelling processes are outstanding right after the Event 2 and Event 3 in which the temperature increases by 12.5°C and 14°C, respectively. It is also noticeable that the weak current is coincident with rapidly rising temperature in the former process. After reaching the maximum, the temperature begins to decrease as the current becomes stronger while the winds are rather weak and variable. Unfortunately the current data is no longer available to be compared with the similar temperature change in the latter process. These results imply that the upwelling effect represented as temperature change is influenced very significantly by other factors than the wind alone. The candidate factors may be the degree of stratification and intensity of the fluctuating TWC. When the cold water mass is waiting close to the surface in the presence of strong stratification with baroclinic tilt-

ing, the temperature change will be immediate and large even under the same wind condition.

A closer investigation reveals that the coastal temperature responds very immediately to wind. Almost respective fluctuation of temperature, small or large, is directly related to wind. The temperature begins to decrease within 3–18 hours after the onset of upwelling-favorable wind. The phase lag between each peak (trough) of wind and trough (peak) of temperature is 12–38 hours. This correlation is inspected in frequency domain by coherence analysis (Fig. 11a). Coherence curve is most significant at periods of 4.0–5.4 days and the corresponding phase difference is 27–37 hours. Another significant peak at 2.4 day-period is likely to be responsible for immediate response of short fluctuations. The phase lag at this period is about 17 hours.

The alongshore velocity is always positive and generally strong whereas the offshore component is much small as a result of the principal component analysis. Alongshore velocity does not seem to be correlated visually with wind. It is very hard to find an indication that a strong wind intensifies the current. Two peculiar events of weak alongshore current may look to be related to the negative wind velocities that happened just before each event. This is not plausible because much stronger winds do not lead to the similar result in this data. The strong velocity over 60 cm/sec is due to TWC having its own variability that might be controlled by some forcing associated with Kuroshio, or by the atmospheric pressure change as explained by Lyu *et al.* (2002). In the frequency domain (Fig. 11b) the coherent low frequencies of periods longer than 20 days is influenced by the sustained strong velocity during the first and second events of upwelling. There is one more coherent band at about 4-day period in which the wind leads the current slightly.

Visual correlation is scarcely detected with ease from the current-sea level and current-temperature relations. Only current-temperature pair seems to show a weak correlation of the strong current and the low temperature during the first two upwelling events. However, Fig. 11d show the inverse coherence only at 4-day period where phase of about 150° should be interpreted as an inverse coherence with 30° phase, that is, increase in positive velocity leads temperature drop by 8 hours. Coherence between current and sea level is substantially low (Fig. 11e). Only periods of 4 and 6 days are of marginal significance having inverse coherence.

Sea level is not correlated well with remaining variables either. Wind is only inversely coherent with sea level at long periods of 30 days or more (Fig. 11c). Sea level-temperature relation (Fig. 11f) is basically the same as current-sea level relation; marginal significance at 12-day and 4-day periods. Phase relation should be understood as a normal coherence of dynamical validity that both variables change in the same fashion. The 4-day period is the only one of significant coherence that is commonly found in all pairs of data in Fig. 11. This period of coherence is also documented in the South Sea of Korea (Lee *et al.*, 2003). As explained by Lyu *et al.* (2002), this periodicity may be related with the variations in atmospheric pressure forcing in the East Sea-Korea Strait system that affects the transport through the strait.

The fact that current and sea level are not closely related with wind or temperature looks perplexing at first. Most of the famous coastal upwelling areas are located in the eastern boundary current regions where current is usually weak and sensitive to wind as described by Smith (1974). The area of present study is under a dominant influence of TWC that is very strong most of the time and has its own variability. With great help from strong baroclinic effect by TWC, the rapid response of temperature would be possible. It is a crucial role of TWC to prepare a background condition of ascending isopleths due to baroclinic tilting. However, TWC itself is so strong that the influence of wind would not be exposed in the analysis.

As discussed by Lee (1983), subtidal sea levels not only vary with same trend at all stations of southeast coast from Busan to Pohang but also do not always show upwelling response to wind. Another finding in this paper is that sea level is not significantly coherent with current either. Sea level variability still remains as a problem to be studied more in the future.

CONCLUSIONS

The observations of current, sea level and temperature were conducted for the investigation of the coastal upwelling process in the southeast coast of Korea in detail by the time series much more refined than daily data used in the previous studies. Coastal temperature and sea level were measured by a tide gauge installed at the coast of Ulsan. A current meter was moored at 20 m depth where the bottom depth was 110 m off Ulsan. Low-pass filtered data were compared with each other to examine the response relations. CTD observation was carried out and sat-

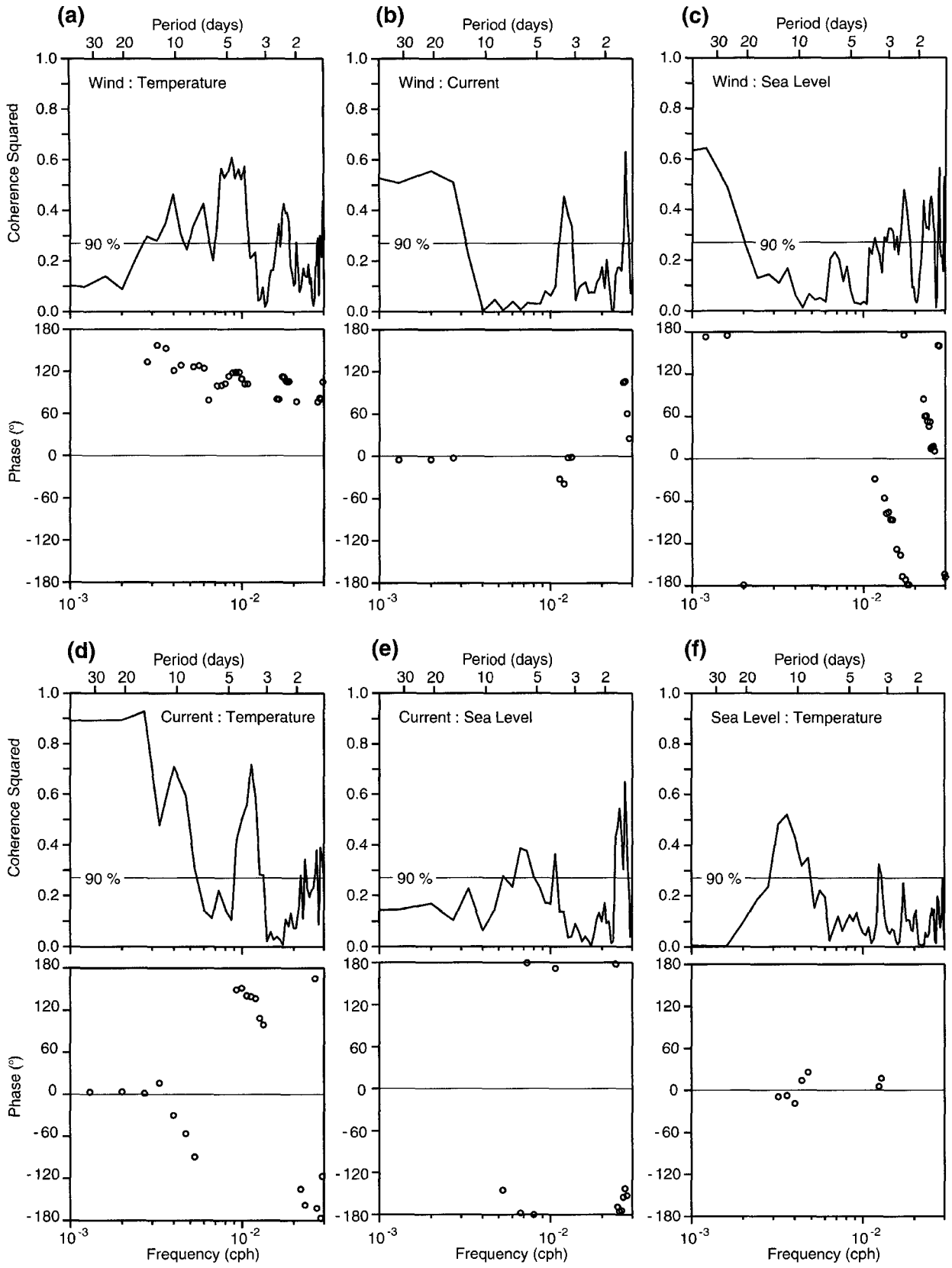

Fig. 11. Coherence analyses of observed variables.

ellite IR imageries were also reviewed.

Southwesterly winds favorable for coastal upwelling dominated the summer of 1997. Besides the numerous cases of small scale upwelling, four major wind events account for 58 days during about one hundred days from June to early September. The most sensitive variable responding to wind variation is the coastal temperature. Time difference between the onset of upwelling-favorable wind and temperature decrease can be as short as 3 hours and the maximum, 18 hours. Coherence analysis of wind-temperature relation informs that there are two significant bands at periods of 4.0–5.4 days and 2.4 days where the respective phase lags are 27–37 hours and 17 hours. Temperature can be lowered below 8°C and maximum decrease is larger than 10°C during an enhanced upwelling. Downwelling process is as vigorous as the upwelling. Maximum temperature increase of 14°C was recorded during 9 days of northeasterly wind in mid-August.

The magnitude of temperature change is not quantitatively proportional to the intensity of wind. Even though the temperature change is very sensitive to wind, its amount also depends on the degree of stratification as well as the dynamic condition of current. Furthermore, current and sea level do not have good correlations with wind or temperature. Current, dominantly to the NNE direction, has average velocity over 60 cm/sec and can be as fast as 100 cm/sec. Because of this powerfulness, TWC has a critical significance of creating and maintaining the rising isopleths toward the coast, whereas the effect of individual response to wind seems relatively negligible to be detected from the temporal variability of current data. Correlations of sea level with other variables are poor as pointed out by Lee (1983). This is not explained clearly in this paper and remains a problem to be explored in the future. However, a coherent band at 4-day period is commonly found in all pairs of variables. The coherence is more significant for wind-current-temperature relations (Fig. 11a, b, and d) than those of sea level with others (Fig. 11c, e, and f).

Our understanding is that southerly wind induces a coastal upwelling but its effect is most evident in the sensitive response of temperature which is dependent on the background condition of baroclinic tilting due to strong TWC near the coast in the presence of developing stratification in summer.

ACKNOWLEDGEMENTS

This research was supported by the Korea Research Foundation through the research program of Korea Inter-university Institute of Ocean Science, Pukyong National University. We appreciate the help of the crew of R/V Tamyang in deploying current meters and CTD observation.

REFERENCES

An, H.S., 1974. On the cold water mass around the southeast coast of Korean Peninsula. *J. Oceanol. Soc. Korea*, **9**: 10–18.

Book, J.W., P. Pistek, H. Perkins, K.R. Thompson, W.J. Teague, G.A. Jacobs, M.-S. Suk, K.-I. Chang, J.C. Lee and B.H. Choi, 2003. Data assimilation modeling of the barotropic tides in the Korea/Tsushima Strait. *J. Oceanogr.* **59**: (submitted)

Byun, S.K., 1989. Sea surface cold water near the southeastern coast of Korea: Wind effect. *J. Oceanol. Soc. Korea*, **24**: 121–131.

Lee, K.B., 1978. Study on the coastal water near Ulsan. *J. Oceanol. Soc. Korea*, **13**: 149–160.

Lee, D.-K., J.-I. Kwon and S.-B. Hahn, 1998. The wind effect on the cold water formation near Gampo-Ulgi coast. *J. Korean Fish. Soc.*, **33**: 359–371 (in Korean).

Lee, J.C., 1983. Variations of sea level and sea surface temperature associated with wind-induced upwelling in the southeast coast of Korea in summer. *J. Oceanol. Soc. Korea*, **18**: 149–160.

Lee, J.C and J.Y. Na, 1985. Structure of upwelling off the southeast coast of Korea. *J. Oceanol. Soc. Korea*, **20**: 6–19.

Lee, J.C., S.-H. Lee, D.H. Kim, Y.T. Son, H.T. Perkins, J.-C. Kim and I.C. Pang, 2003. Circulation in the South Sea of Korea in Spring 1999. *J. Korean Soc. Oceanogr.*, **38**: 143-155.

Lyu, S.J., K. Kim and H.T. Perkins, 2002. Atmospheric pressure-forced subinertial variations in the transport through the Korea Strait. Geophys. Res. Lett., 29: 10.1029/2001GL014366.

Smith, R.L., 1974. A description of current, wind and sea level variations during coastal upwelling off the Oregon coast, July-August 1972. *J. Geophys. Res.*, **79**: 435–443.

Teague, W.J., G.A. Jacobs, H.T. Perkins and J.W. Book, 2001. Tide observations in the Korea-Tsushima Strait. *Cont. Shelf Res.*, **21**: 545–561.

Manuscript received July 21, 2003
Revision accepted September 15, 2003
Editorial handling: Sang-Ho Lee